Undergraduate Honors Theses   Theses, Dissertations, & Master Projects

5-2015

Growth and Characterization of Gold Nanostructures Produced from Diatomaceous Algae

David A. Specht
College of William and Mary

Follow this and additional works at: https://scholarworks.wm.edu/honorstheses

Part of the Biological and Chemical Physics Commons, and the Condensed Matter Physics Commons
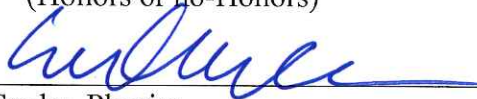
Recommended Citation

Growth and Characterization of Gold Nanostructures Produced from Diatomaceous Algae

A thesis submitted in partial fulfillment of the requirement
for the degree of Bachelor of Science in Physics from
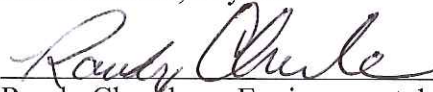The College of William and Mary

by

David Specht

Accepted for ___HONORS___
(Honors or no-Honors)

Bill Cooke, Physics

Gina Hoatson, Physics

Randy Chambers, Environmental Science & Policy

Williamsburg, VA
May 5, 2015

Growth and Characterization of Gold Nanostructures Produced from Diatomaceous Algae

David Specht, Advisor: Bill Cooke

May 11, 2015

Abstract

Silica nanostructures (frustules) grown by the algae *Thalassiosira eccentrica* can be used to template the production of regular arrays of supported gold nanodots, with sizes ranging from 30 to 50 nm. This growth is of particular interest because it represents a novel and efficient way to produce and distribute nanoparticles, particularly for applications in catalysis, and may demonstrate a value for a byproduct ash produced when diatomaceous algae is used to produce biofuel. Growth has been characterized by both SEM and AFM imagery. This growth of regular nanoparticles has also been demonstrated with carbon evaporation, and may be a means to produce similar structures using a diversity of materials. This research explores the explanation, replication, and potential applications of this phenomenon.

Contents

1   Introduction

Diatomaceous algae produce intricate silica nanostructures called frustules (see, for example, Figure 1). These structures have great potential as templates for nanostructured materials [1, 2, 3], due to their complex hierarchical structure, nanoscale surface features, inexpensive production, and incredible species and morphological diversity.

In this study, I have demonstrated that gold sputter-coating can be used to produce patterns of nanoparticles using some *Thalassiosira* spp. diatoms as templates and support structures. Under sputter-coating, gold will nucleate as dots on the silica surface in partially ordered patterns (see Figure 2 as an example). Average dimensions of these nanodots range from 30 to 50 nm across, although with particle uniformity across single diatoms. The patterns have also been demonstrated to result after carbon evaporation.

The resulting described features were characterized using Scanning Electron Microscopy (SEM) and Atomic Force Microscopy (AFM) techniques. The nanoparticle growth likely is the result of micro-indentations in the diatom surface, as revealed by the AFM. This method of producing dispersed metallic nanostructures that independently nucleate on a support surface via sputter-coating of these diatom templates is novel. Previous studies, for example, have used electroless gold plating or evaporation to create full replicas of diatoms [2, 4], or attached prefabricated nanoparticles to frustules [5].

So far, this particular result of regular nanodots has only been observed with *Thalassiosira* spp. diatoms. However, given the very great morphological diversity of diatoms (in addition to other biosilica nanomaterials), it is very likely that similarly interesting regular nanostructures will result from this method of coating for a great number of algal morphologies.

This research project originates from work done for the York River Algae Project. The purpose of the York River Algae Project [6, 7] is to explore wild farming of algae for remediation of water pollution and for biofuel production. Fuel production using
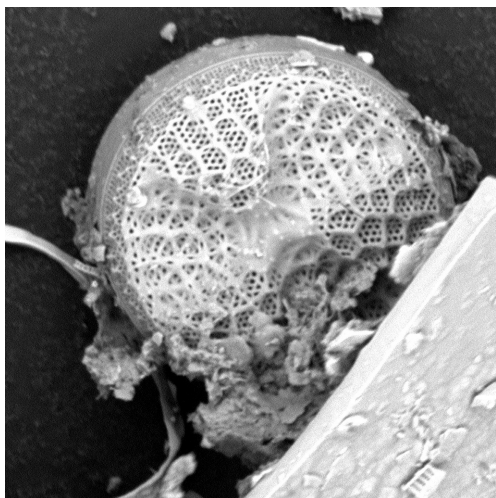
Figure 1: Sample of complexity of the diatom structure. This entire structure is 20 μm across. There is an external structure (called the foramen) with larger pores and a lower finer structure which lies against the cell membrane called the cribum.

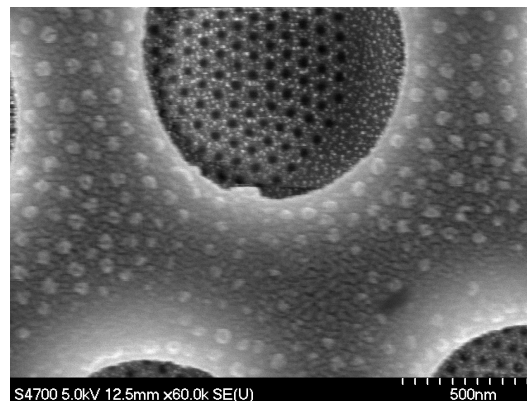S4700 5.0kV 12.5mm x60.0k SE(U)   500nm

Figure 2: Sample of nanoparticle features grown on a *Thalassiosira sp.* diatom. Particles seem to have pooled on both the foramen (the larger particles on the upper structure) as well as the cribum (the smaller particles on the lower structure).

diatomaceous algae produces a waste ash product dominated by frustules. The purpose of this work was to explore possible applications of this ash product. Although this research explores a phenomenon for a specific *Thalassiosira* species, it may lead to development of a bulk nanostructure production process utilizing this high-grade ash. A high-value application for this ash may increase the viability of this algae production strategy.

Supported metallic nanostructures, including gold, have many potential applications. Further development of this technology may represent a useful way to produce quantities of supported gold nanoparticles, control their size, and efficiently distribute them on a substrate, particularly for applications in catalysis. Other potential applications of this phenomenon could include Surface-Enhanced Raman Spectroscopy or bulk production of nanoparticles (if the frustule structure is removed) for applications like 3-D printing of metals. Since this phenomenon is not restricted to gold, or even to metals (this was

also demonstrated with carbon evaporation), these frustules could represent a universal template for supported arrays of nanodots made from numerous or even multilayered materials.

1.1 Diatomaceous Algae

Diatomaceous algae are composed of diatoms, unicellular photosynthetic organisms that have an underlying silica skeletal structure called a frustule. Diatoms are extraordinarily diverse, with over 200,000 estimated species [8]. Diatoms have evolved a correspondingly wide variety of frustule morphologies inresponse to a diversity of environmental conditions. The frustule protects the diatom from predation, mechanical damage such as abrasion, and changes in osmolarity [3].

Diatomaceous earth, the fossil remains of frustules mined as diatomite, has diverse existing applications. Diatomaceous earth is heavily used as a water filtration medium, and is also used as a filler, mechanical insecticide, and soil additive. Famously, Alfred Nobel used it as a stabilizer for nitroglycerin, producing dynamite. Since the fossil remains of diatoms have so many diverse applications, a similar but higher-grade product derived from live diatoms may also have diverse applications.

Diatoms have interesting nanotechnology applications, including possible applications in biophotonics, medicine delivery, and computing [8]. Diatoms have many interesting inherent properties which lend them towards applications in physics. For example, these organisms can function as microlenses [3]. Their complex nanoscale hierarchical structures (Figure 1) are suited to applications in filtration or catalysis, and the silica structures can be replicated in active materials for particular applications, such as gold [9]. Production of microstructured materials via diatom templates could exploit their exponential growth for rapid fabrication, as an alternative to lower throughput methods such as photolithography [8].

Diatom frustules are composed of two halves (called valves) bound together with a
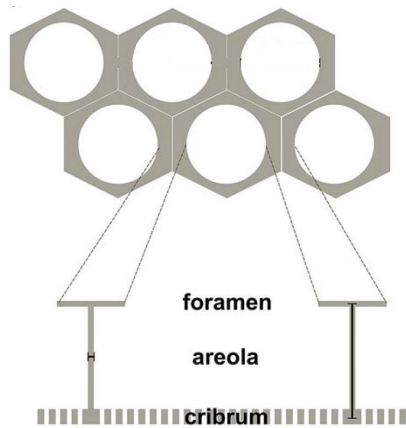
Figure 3: Diagram of frustule pore structure, adapted from [10].

Figure 4: Conglomerate ash product resulting from York River Algae Project biofuel production.

midsection called the girdle band. The diatoms that are primarily studied in this thesis possess a pore structure on the outer face of the valve, as diagrammed in Figure 3. The primary upper structure is larger honeycomb called the foramen [10]. There is then a lower second layer with much smaller perforations, called the cribum (or sieve plate). The cribum and foramen form the top and bottom of hexagonal chambers called aerolae. As shown in Figure 3, T-shaped silica structures support the foramen above the cribum.

1.2 York River Algae Project

Algal biofuels are a promising source of carbon-neutral and domestic fuel, but current commercial land-based methods used to grow them are inefficient and costly. According to the National Academy of Sciences, algal biofuel production sufficient to meet only 5% of US transportation needs would place unsustainable demands on energy, water, and nutrients [11]. Without major innovation, the requirements of land-based algal biofuel production would essentially negate any environmental benefits and be an inefficient

source of fuel on a large scale.It is estimated that the nutrient demands for producing algal biofuels meeting 5% of the United States' transportation demands would require an additional 44 to 107% of current nitrogen use and 20 to 51% of current phosphorus use, using current methods [11].

The York River Algae Project [6, 7] is a means to develop the potential of algae biofuels while avoiding these issues by growing wild algae in already eutrophic waters, such as the York River. The algae used in this study were grown on vertical screens suspended in the York River by a 10 meter barge called the York River Research Platform (see Figure 5). This system was built as a test platform for study before construction of a planned 1 acre pilot farm. While land-based algae production requires the supply of water, nutrients, and carbon dioxide, these resources are readily accessible to algae farmed naturally in the York River. The purpose of this work is also water quality remediation, as pollution due to excessive nutrient runoff from the Chesapeake Bay watershed would be lessened by large-scale algae farming.

One issue with producing algae biofuel in this way is that the species grown cannot be selected in advance, and are subject to seasonal and environmental changes in species dominance. In land-based racetrack or bio-reactor systems, although comparatively inefficient, species of algae can be selected for higher oil content or for lower byproduct mass. The purpose of this study is to evaluate the potential usefulness of diatomaceous algae, which are grown abundantly in the York River but have a high byproduct mass. These algae are suited for pyrolytic gas to liquid biofuel production. Pyrolisis is used to produce fuel from the algae but produces an ash byproduct, dominated by a mixture of skeletal remains of diatomaceous algae and clay particles.

Over 75% of the algae biomass produced by this method becomes ash [7]. Originally, the purpose of this research was to characterize and explore applications for this ash product by developing an application for it and therefore increase the viability of a renewable and environmentally friendly energy technology. Although this thesis deals
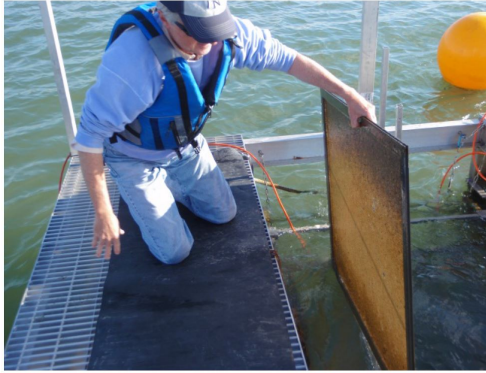
8

Figure 5: Removal of algae-laden screens from the York River Algae Project raft.
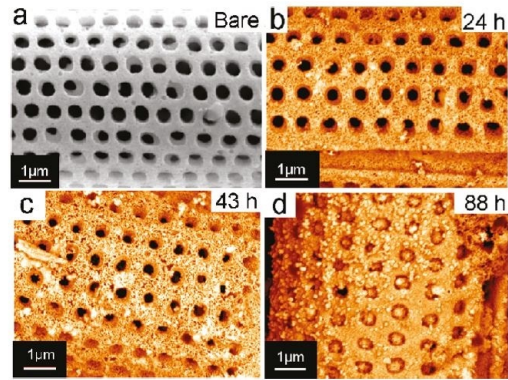

Figure 6: SEM images showing the growth of diatom gold replicas, from [2].

primarily with the effect on the frustule of one *Thalassiosira* species (present in the York River), it is likely that there is value in the bulk product of the frusule ash under coating for nanoparticle growth.

1.3 Gold Nanostructures

Nanoscale clusters have unique physical and chemical properties not present in bulk material [12]. The electronic structure of atoms, molecules, and bulk solids has been studied exensively, but important work remains to be done in the exploration of 'embryonic' materials made from clusters of atoms. An understanding of this size-dependence effect is critical for applications utilizing chemical and catalytic properties. Experimentally, these structures need to be studied locally or via some form of size selection in order to elicit the size-dependent properties.

Gold nanoparticles have potential in many applications. Nanocrystal confinement of electrons represents the most effective means to control the electronic, optical and magnetic properties of solid materials [13]. Despite the fact that bulk gold is relatively inert, gold nanoparticles are catalytically active, even at lower temperatures, lending them to applications in energy efficient processes [14]. Gold nanoparticles have medical

potential, such as for photothermal cancer treatments, non-invasive diagnostic imaging, and targeted drug delivery [15].

Catalytic and optical properties desirable for such applications are tunable as a function of particle size and shape [16]. In surface-enhanced Raman scattering applications, Au nanocrystal structure determines the number, position, and intensity of localized surface plasmon modes [13]. In catalysis applications, the catalytic capability of Au is driven by very low-coordinated atoms, so the prevalence of corner and edge sites is important [14]. Size control also is critical in many of these applications. The catalytic properties of gold particles can be dramatically influenced by particle size [14]. As a result, it is desirable that synthesis routes promote formation of particles of predictable size and shape, with limited post-processing.

Use of diatoms as a template for metallic nanostructures is not a new idea. For example, Losic et al. [4] have replicated entire diatom structures in gold (see Figure 6, from [2]). The diatom is heavily coated such that the metallic structure is self-supporting, and the silica template is dissolved to leave a double-walled inverse of the diatom structure. While this does produce interesting and porous metallic structures suitable for catalysis, this is a relatively inefficient way to use the gold, as the outer surface plays the primary role. Another approach has been to use nanoparticles to uniformly decorate the diatom shape, using the diatom as a support structure. See, for example, [5]. While this may be an efficient way to distribute nanoparticles, it doesn't clearly take advantage of the diatom's shape.

1.4   Supported Gold Catalysts

Despite the longstanding belief that gold was too inert to have any catalytic activity, gold nanoparticles have immense catalytic capability not present in bulk gold [17]. Bulk gold is noble because there are high activation barriers for dissociating small molecules and low adsorption energies. Suprisingly, nanogold is a great catalyst.

The oxidation of carbon monoxide by oxgen is model reaction for the utilization of nanocatalysts [12, p. 91]. Although the CO combustion reaction $2CO + O_2 \rightarrow 2CO_2$ is exothermic, the reaction will not proceed in the gas phase under ambient conditions due to a large energy barrier due to the strength of the oxygen molecule's bond. Breaking of this oxygen bond is achieved by metal catalysts, and the reaction proceeds at the surface of the catalyst between CO and O particles.

Pure gold nanoparticles, although relatively easy to study in the gas phase, are also not a practical catalyst, as they will aggregate with time. A support structure is needed to immobilize the nanoparticles over a large surface area. Few examples of materials made up of regular arrays of individual clusters have been reported so far [12, p. 51]. Catalysis by gold aggregates on oxides are of great significance, but the process underlying low-dimensional gold catalysis on these surfaces is not yet well understood.

Deposition of prefabricated gold clusters onto MgO films for catalysis of CO to CO_2 is a model for supported gold nanoparticles as catalysts [12, p. 117]. Without the gold, no reaction proceeds at the MgO surfaces. Gold clusters are deposited on both defect rich and defect poor MgO films. Substrate defects in the MgO are critical for size-dependent catalysis using gold clusters, as gold clusters are observed to be inert on defect-poor films. The gold clusters bind to F centers, vacancies of the anion in the crystal structure. Gold clusters bound to these F centers highly activates molecules for catalysis. There are also size-dependent effects with respect to cluster/support interaction, dynamics of clusters on the surface, size dependent migration and coalescence of clusters.

The electronic structure of small metal clusters varies as a function of the cluster size. Effects are greatest for compounds with 1 electron in the s orbital (e.g. gold). Quantized electronic structure results in even/odd variability of electron binding energy (Figure 7). Catalytic activity of clusters is therefore very sensitive to cluster size - even when changed by just a single atom [12].

Because of their high surface area with respect to total volume, diatoms are ideal
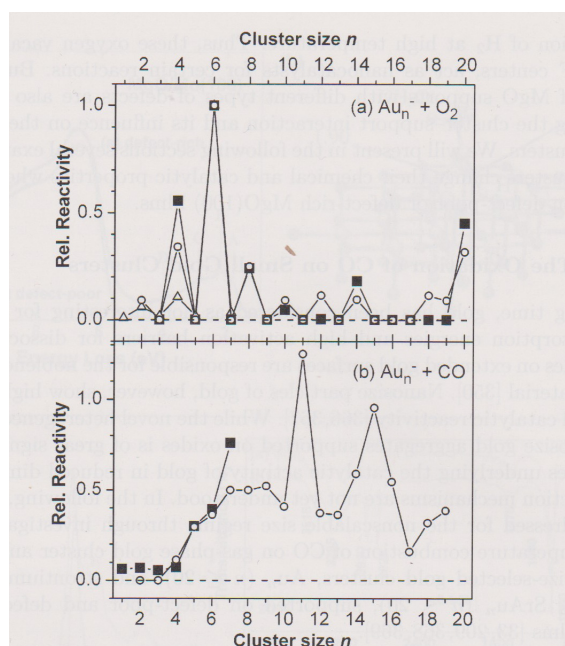
11

Figure 7: Alternating reactivity for the $CO \rightarrow CO_2$ reaction as function of gold cluster size. Figure from [12].

for such a support. Diatom-derived nanomaterials (e.g. as pictured in Figure 6) have already been demonstrated to be useful in catalysis, for example by Losic et al. in reduction of 4-nitrophenol to 4-aminophenol with sodium borohydride as a reductant [2], as pictured in Figure 8.

1.5   *Thalassiosira eccentrica*

The bulk of this research deals with gold nanoparticle arrays on the frustules of *Thalassiosira eccentrica*. This centric diatom is present in marine waters throughout the world, with a species distribution ranging from Antarctic to tropical waters. The species derives its name from scattered pores on the surface of the foramen with eccentric spacing.

It is probable that they are not all one species [18]. Rather, Thalassiosira Eccentrica may just be a catch-all for Thalassiosira that have this irregular pore pattern, especially as the species distribution ranges from Antarctic to tropical waters. Several other dif-
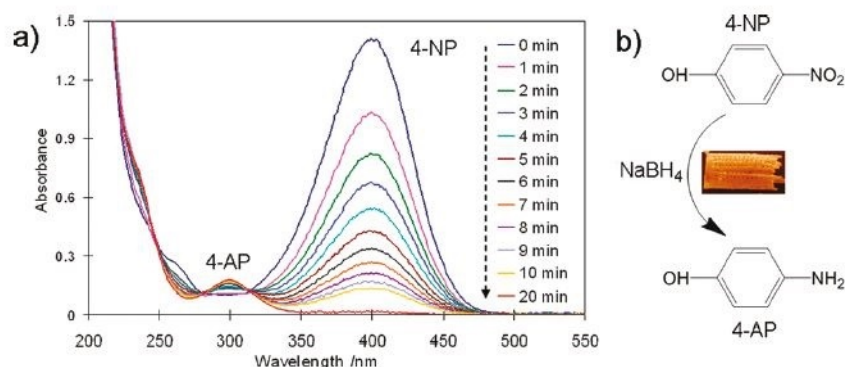
Figure 8: Time-dependent absorption spectra for the catalytic reduction of 4-nitrophenol to 4-aminophenol using gold diatom replicas. Figure from [17].

ferent species (e.g. *T. mendiolana*) seem to be very difficult to differentiate from *T. eccentrica*. *T. mendiolana* is more thinly silicified, with differences in pore distribution that is are "too difficult to quantify to be useful"[18]. There are also many different variants for this same species, like *Coscinodiscus eccentrica*, *Thalassiosira excentrica*, etc.

T. eccentrica is extremely tolerant of variable water temperatures. At the time [18] was written, temperature limits had not been established. *T. eccentrica* is believed to be fairly common on US West and East coasts, and in European waters.

1.6   Sputter Coating

In Scanning Electron Microscopy (SEM), a conductive metal coating (frequently gold or gold/palladium) is used routinely to increase the surface conductivity of a sample to prevent charging during imaging. Sample charging is a major limiting factor in imaging of nonconductive biological materials. Charging is caused by charge buildup in a nonconductive sample as electrons deposited by the SEM electron gun cannot reach the grounded sample holder and remain on the sample surface. This causes imaging defects which limit the achievable image resolution.

13

Sputter-coating works by bombarding a sputter target made from the desired deposition material (e.g. gold, carbon, or silver) with ionized gas particles (argon) in a chamber such that the deposition material is ejected (sputtered) onto the sample surface. In this way, thin films of these materials can be grown on the diatom frustules.

2 Preparation of Diatomaceous Supported Gold Nanostructures

Sputter coating of diatoms for imaging purposes of the York River Algae Project resulted in the discovery of interesting patterns of gold nanostructures growing on the diatom surfaces. Most gold growth (See Figure 9) is relatively uninteresting island growth. However, under certain coating conditions and for certain species, growth would be guided by the structure of the frustule below, creating potentially interesting gold nanostructures (See Figure 10).

Most interestingly, it was found that a certain diatom created patterns of regular similarly-sized gold nanoparticles in a lattice-like structure. These patterns will appear on either the cribum or foramen, and sometimes both (as in Figure 2). The diatom substrate it was found on appeared to be of a *Thalassiosira* species [19]. This particular phenomenon has since been repeated irregularly for this species of diatom, which appears irregularly in samples from the York River. So far, patterning like this has not been observed in any of the other species drawn from the York River, but is reproducible on this species of *Thalassiosira*.

Through the beginning of 2015, York River algal material was used in research of this gold growth phenomenon. Research was done into better cleaning methods and size-selection techniques to try and isolate the *Thalassiosira* species of interest. The species naturally occuring in the York River vary wildly by collection site and the time of year, making it extremely difficult to produce samples with the *Thalassiosira* species reliably present. Concerned that I may not be able to study the nanoparticle growth
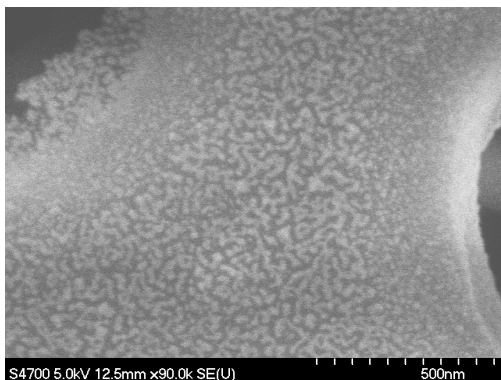
Figure 9: Gold growth on a diatom of unknown species. There is relatively uninteresting island growth at the surface.
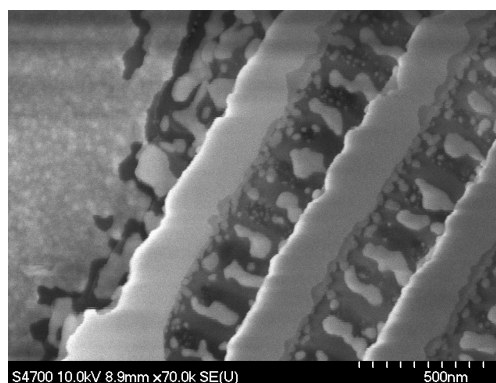

Figure 10: Gold/palladium growth on a *Berkeleya* diatom. The growth is adopting a pattern guided (to a degree) by the underlying structure of the frustule beneath it.

phenomenon, I explored applications of growth on bulk frustule material that wasn't a species-specific effect.

Without a sample purely composed of *Thalassiosira*, it proved very difficult to study the Figure 2 gold growth phenomenon of interest. At length, the organism was (tentatively) identified as *Thalassiosira eccentrica*. A purchased monoculture of this species showed the same nanoparticle growth characteristics of the York River *Thalassiosira*.

Subsequent research has used this *T. eccentrica* monoculture to study the gold nanostructure growth. In this section, I describe the initial attempts at isolation from York River samples, as well as the eventual more standard procedure using the *T. eccentrica* monoculture.

2.1 Isolation & Culturing

Samples of wild algae were collected from the York River and surveyed for *Thalassiosira* or other diatoms that showed interesting characteristics under sputter-coating using electron microscopy. Initially, dried material from the York River Algae Project (e.g.
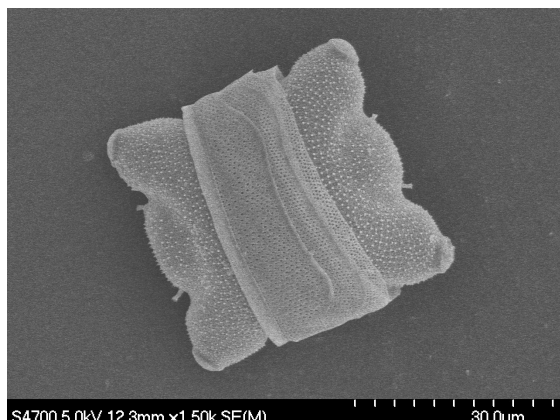
15

Figure 11: Full *Odontella sp.* diatom isolated from material grown in the York River using size-selection techniques.
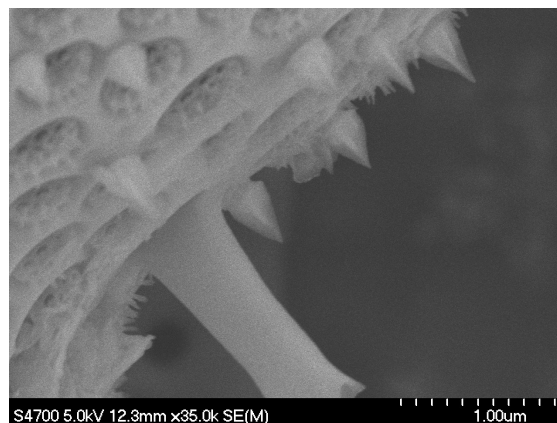

Figure 12: Exterior structures of an *Odonotella sp.* diatom. These very thin and sharp structures may be an ideal surface for growth of a supported catalyst.

Figure 4) was used. However, these sample materials were of very poor quality because they were dominated by fragments of diatoms (oven drying seems to cause them to break), were difficult to clean, and agglomerated into larger clusters that were more difficult to image with the electron microscope. I transitioned to using material grown on screens suspended in a York River boat dock, which were collected and preserved in ethanol.

A sample of diatoms from the York River may have roughly twenty to forty different morphologies present. To improve the homogeneity of gold nanostructures grown from these frustules, I attempted to isolate diatoms of interest using size-selective filter media (See Section 2.2 for this procedure).

Unfortunately, although the *Thalassiosira* diatom of interest (pictured in Figure 13) seems present in samples from almost all locations and at all times of year from the York River samples, it has an extremely low density in samples and falls within a similar size range of other diatoms that are present.The size selection did succeed in increasing its prevalence in samples, but failed to isolate it sufficiently for regular study.

In this size-selection process, I did accidentally succeed in isolating *Odontella sp.* diatoms instead (see Figure 11). This diatom has structures (see Figure 12) which may also be of interest as a support structure for gold nanostructures, and will likely be the subject of future investigations.

The easier alternative to isolating the diatom of interest from York River samples may be to culture it in the lab from monocultures available for purchase. However, the many species of *Thalassiosira* available for purchase only represent only a small fraction of the species in the wild. Additionally, it had proven difficult to identify this particular *Thalassiosira*. Although I had many images of the cleaned or coated frustule, I did not have images of the live diatom, which are more commonly used to do the identification.

I attempted to identify the diatom myself, and guessed that our diatom may be *Thalassiosira decipiens*. However, this was an incorrect identification (compare Figures 15 and 16 with Figure 13). According to [18], the live *T. eccentrica* is commonly confused with *T. decipiens*. I now have a live sample of a monoculture purchased from the NCMA (National Center for Marine Algae) of *T. decipiens*. It is possible that this diatom may also yield some interesting nanostructure under coating and has been kept alive. I also studied *T. weissiflogi*, which is cheaply available as aquaculture feed, on the chance that it may also yield interesting nanostructures.

I contacted a number of people who were unable to definitively identify the diatom at more than the level of *Thalassiosira*. However, a contact at the NCMA directed me to get in touch with Andrew Alverson at the University of Arkansas, who tentatively identified this algae of interest as *Thalassiosira eccentrica*, although he said he could not be positive without an image of the inner valve face. This identification was made due to the presence of eccentrically spaced pores on the outside of the valve (see Figure 14).

Samples of *T. eccentrica* were purchased from the Culture Collection of Algae and Protozoa (CCAP) in Scotland. The sample was originally collected in the Bay of Fundy, Canada, in 2010. Optical and SEM images of *T. eccentrica* from this culture are inluded
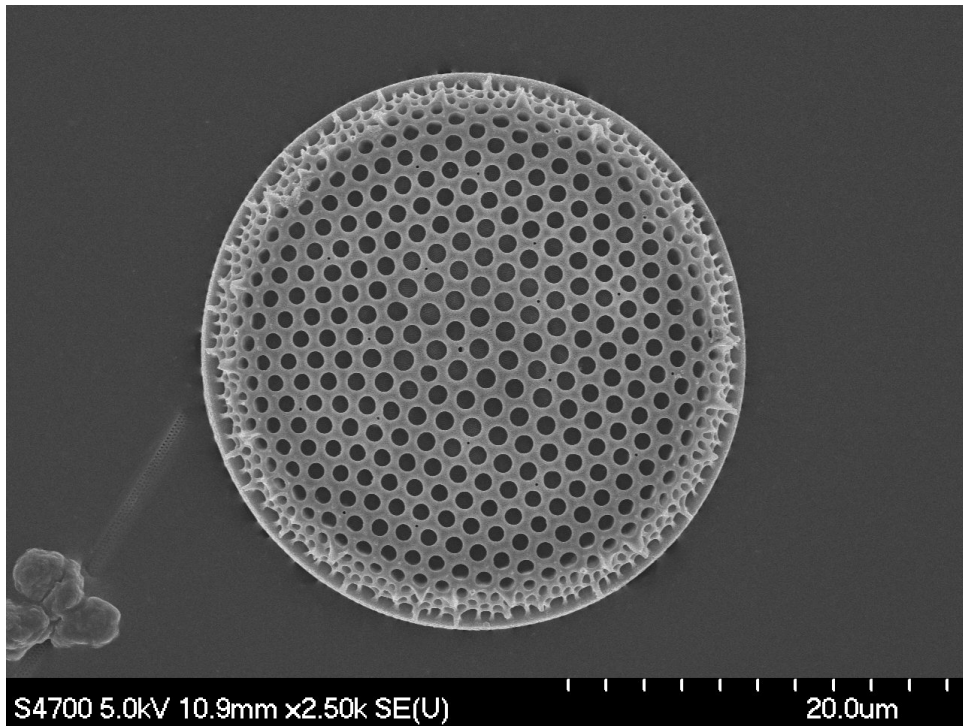
Figure 13: Full size image of the York River *Thalassiosira* species used to make the species identification of *Thalassiosira eccentrica*.

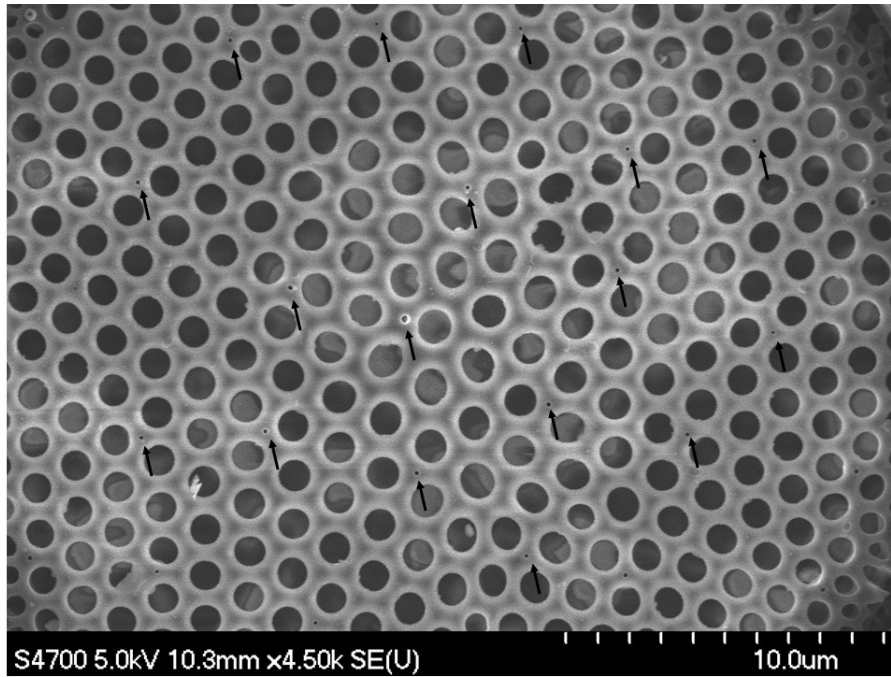Figure 14: Arrows indicating location of 'eccentric' pore spaces indicative of *T. eccentrica*

Figure 15: Whole *Thalassiosira decipiens* diatoms. At such low magnification, these are plausibly similar to the *Thalassiosira* of interest.
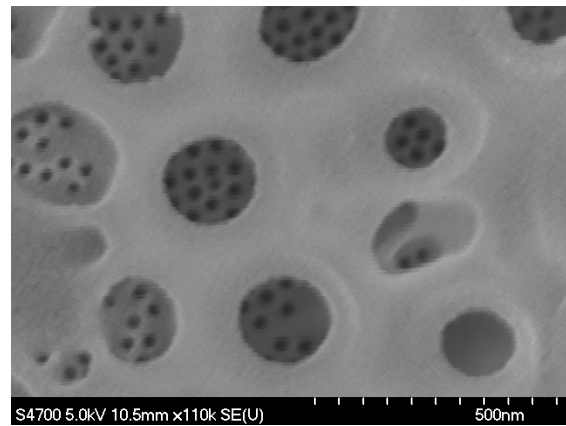

Figure 16: Upon closer inspection, the foramen and sieve plate structure of the *Thalassiosira decipiens* diatom is very different than the York River *Thalassiosira* of interest.
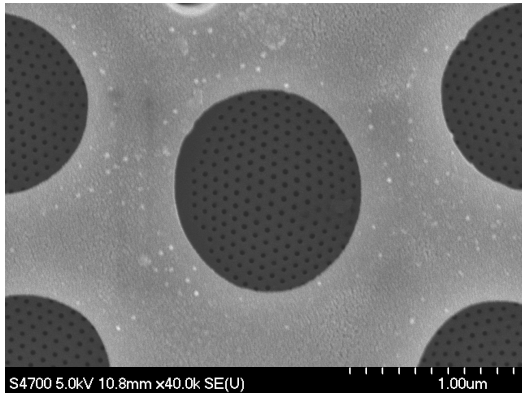
Figure 17: Minimally coated image of the York River *Thalassiosira* species foramen and cribum used to make the species identification of *Thalassiosira Eccentrica*.
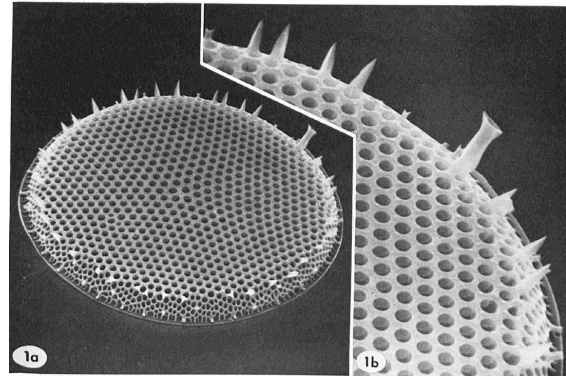

Figure 18: Identfiication plate of *T. eccentrica* from [18].

in Figures 19 and 20. As the cleaning causes heavy losses, it is necessary to maintain a volume of diatoms to work with, so I am exploring culturing larger volumes from the samples that I have. The current culture is being maintained under grow lights in accordance with instructions from the CCAP.

f/2 culture media is used to grow *T. eccentrica*. This media contains saline water and a mix of nutrients required for algal growth (particularly silica needed for frustule growth). See [20] for the recipe of this medium.

Unfortunately, *T. eccentrica* may be difficult to culture in the lab, despite its hardiness in the wild. The NCMA, which previously had a culture of it, was unable to keep it from dying in captivity. The sample is alive, although it is growing extremely slowly.

2.2 Diatom Cleaning

I use hydrogen peroxide to strip the organic matter from the surface of the frustules in preparation for coating and imaging. The method is derived from that described in [21]. In that procedure, however, I found that the boiling action of the hydrogen peroxide
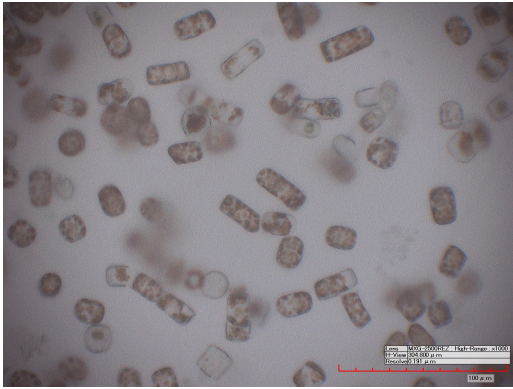
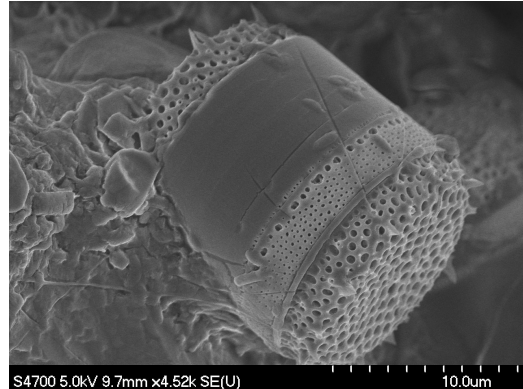Figure 19: Optical imagery of *T. eccentrica* from the CCAP monoculture.

Figure 20: SEM imagery of a whole *T. eccentrica* from the CCAP monoculture.

was too aggressive and shattered most of the whole diatoms in the sample. Instead, I have found that running hot hydrogen peroxide through a diatom sample over a plastic sieve produces the desired result with minimal losses of diatoms. This method is used for both samples collected from the York River platform and material cultured in the lab.

The apparatus used to do this is shown in Figure 21. The top sample holder, filter apparatus, and clamp are from a Millipore vacuum filter assembly. The evacuated flask used in vacuum filtration has been replaced with a graduated cylinder, and no vacuum is used during the cleaning. I have replaced the filter media usually used for vacuum filtration with a 10 μm plastic filter, supported by a metal mesh disk that is part of the Millipore apparatus.

In this procedure, I extract roughly 1 mL of live or preserved diatoms in water and put this onto the plastic sieve material in the sample holder. I then heat 25 mL of hydrogen peroxide to 80 C and periodically flush this hot hydrogen peroxide through the diatoms in the sample holder over a period of 15 minutes. After the hydrogen peroxide is used up, I then rinse the diatoms with distilled water and the sample is ready to be

Figure 21: Apparatus used to flush diatoms with hot hydrogen peroxide.

Figure 22: Modified sample tabs for imaging with both SEM and AFM. The assembled tab is on the left, and the disassembled components are on the left.

mounted for imaging. I then mount samples by lightly tapping the SEM carbon tabs (conductive carbon pads used for SEM mounting) against the sieve.

In the York River samples, I attempted to size-select diatoms using a series of plastic sieve media. Although this succeeded in isolating an *Odontella* species, it was not sufficient to isolate the *Thalassiosira* of interest.

2.3 Coating

Sputter-coating is used to produce nanostructures at the surface of the cleaned frustules. In the standard procedure, samples are mounted on carbon SEM tabs and sputter-coated with gold using a Hummer sputter coater. Deposition rate is controlled by keeping the tabs a standard distance from the sputter target by using a stage and maintaining a

near constant current in the device. Typical coatings range from 30 seconds to several minutes. This procedure has also previously been done using carbon evaporation instead of sputter-coating.

For the primary results of this thesis, gold coatings of 30 seconds, 45 seconds, 1 minute, 3 minutes, and 6 minutes were applied to *T. eccentrica* frustules and then imaged with the SEM (all samples) and AFM (0 and 30 seconds) to study nanoparticle growth.

2.4 Imaging

Samples prepared in this fashion were then imaged using SEM and AFM techniques. Throughout this project, SEM has been the primary tool for studying the growth of these nanostructures and assessing the quality and types of diatoms present. For the primary results of this thesis, *T. eccentrica* diatoms were sequentially coated and then imaged in order to observe the growth of nanoparticles as a function of sputtering time. The SEM primarily used is a Hitachi S-4700 Field Emission SEM.

In this procedure, a goal has been to return to the same frustules between coating and imaging steps in order to study the nanostructure growth on individual diatoms. Until recently, it has not been possible to transfer the same samples between the AFM and SEM in the ARC lab. A hybrid sample tab (courtesy of Reed Beverstock) that is capable of making the height clearance of the AFM and accomodating the grounding and sample holder requirements in the SEM was built (See Figure 22). There is a notch in the surface of the sample tab so that the orientation of the tab can be restored as one moves between devices and so that the same sample can be located.

There are several important steps for good SEM imaging of these samples. Samples need to be sparsely distributed on the sample tab, with no overlap. Overlapping diatoms prevent proper grounding against the carbon substrate. Additionally, certain parameters for the SEM imaging have been very important. Particularly, lower accelerating voltages

need to be used in order to image minimally conductive samples. Generally, for images with 30 seconds or less of gold coating, an accelerating voltage of 1.5 kV was used, versus 5 kV for more heavily coated samples.

The primary difficulty in AFM imaging has been locating suitable diatoms in the AFM's optical camera. Not only are the diatoms quite small, but the cleaned frustules are transparent under the lighting in the AFM optical camera. In order to deal with this problem, the locations of suitable diatoms were mapped using an optical microscope. Samples are found on the AFM by locating larger landmarks (creases in the carbon tab, bubbles, etc.) on the steel surface of the sample tab and using information from the optical imagery to infer the diatom positions.

It is critical to be able to map out the position of the diatoms on the sample, not only to be able to return to the same one for imaging, but so that the AFM tip doesn't come into contact with the carbon substrate. The AFM tip is very sensitive and is vulnerable to getting stuck in the sticky carbon tabs, so it must touch down on the hard silica surface. For the same reason, it is important that the diatoms be well cleaned such that the tip doesn't become fouled in biological residue at the surface of the diatom.

3   Results

Results from throughout this semester and this project that are relevent to the overall goal of studying and understanding the production of these nanostructures are included here. The primary results describe how the cultured *Thalassiosira eccentrica* diatoms respond to sequential coating. Achieving this series of images of the resulting gold nanoparticle structures has been the final goal of this thesis.
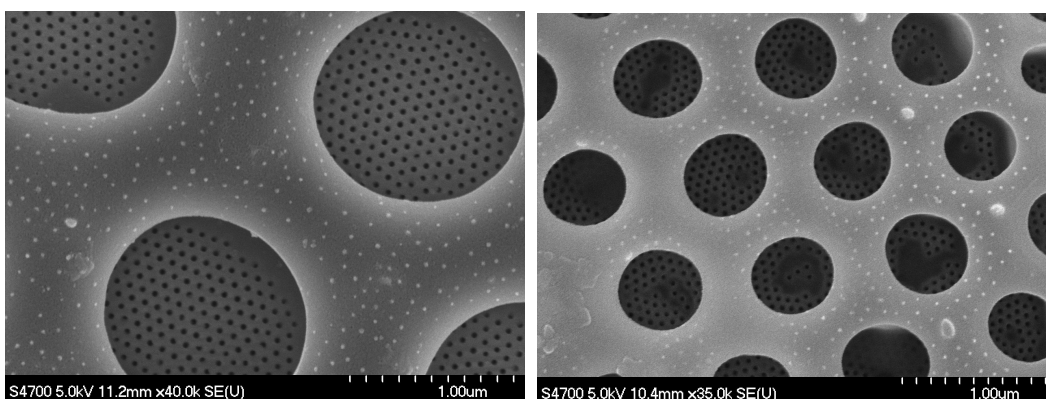
Figure 23: Growth of gold nanoparticles on the foramen of the *Thalassiosira sp.* from the York River. Compare with Figure 24.

Figure 24: Growth of gold nanoparticles on the foramen of the cultured *Thalassiosira eccentrica* (45 seconds of coating). Compare with Figure 23.

3.1 Scanning Electron Microscopy of Supported Gold Nanostructures

York River *Thalassiosira* diatoms were observed to form arrays of gold nanoparticles under gold sputter-coating (See Figures 2 and 23). This phenomenon was observed to occur on both the cribum and foramen.

This phenomenon has also been replicated for *T. eccentrica* diatoms grown from a monoculture, although so far this has only been observed on the diatom foramen. The distribution of particles observed on the foramen is comparable between the two specimens: compare Figures 23 and 24.

SEM imagery of the sequential coating of *T. eccentrica* diatoms is included in Figures 25, 26, 27, 28, 29, and 30. Imagery of 0 seconds, 30 seconds, 3 minutes, and 6 minutes of coating are included.

In Figures 25 and 26, the *same diatom* is imaged between sequential stages of coating. I will refer to it as the *T. eccentrica* standard. Additionally, this *T. eccentrica* 'standard' diatom is the same diatom as imaged in Section 3.2 via the AFM.

Odontella sp. diatoms (Figure 11) did not seem to respond to coating in a fashion as
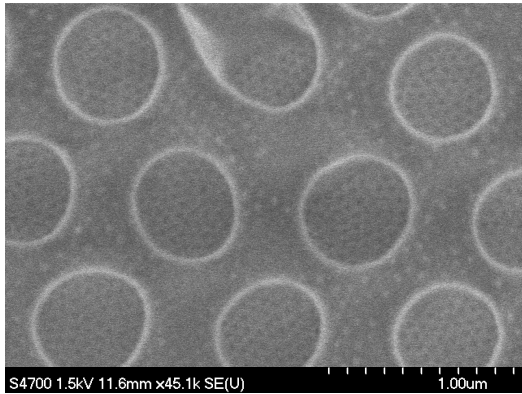
Figure 25: SEM image of the foramen of *T. eccentrica* standard diatom with no gold coating. Features corresponding to future sites of gold nanoparticle growth are visible.
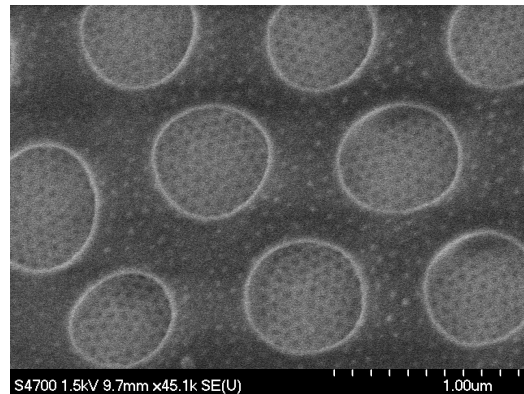

Figure 26: SEM image of the foramen of the *T. eccentrica* standard diatom with 30 seconds of gold sputter. The SEM image does not look all that different from the uncoated diatom- although the difference under the AFM is dramatic.
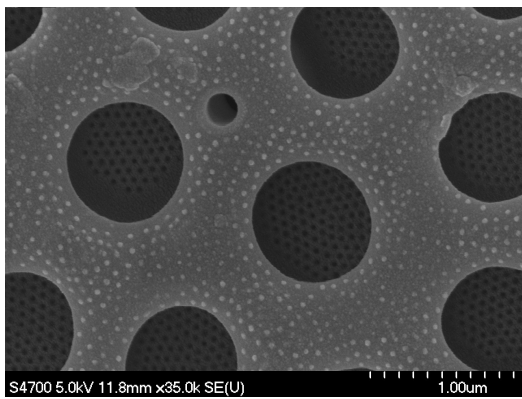

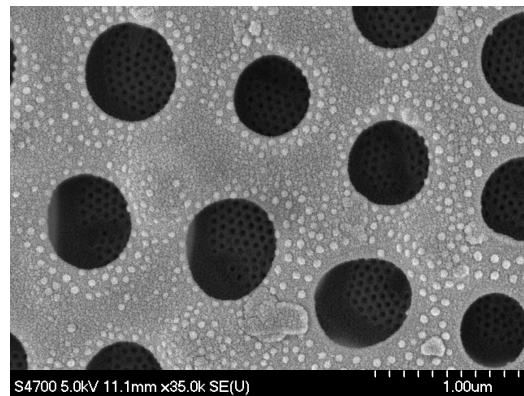Figure 27: SEM image of 3 minutes of gold growth on a *T. eccentrica* diatom.

Figure 28: SEM image of 6 minutes of gold growth on a *T. eccentrica* diatom.
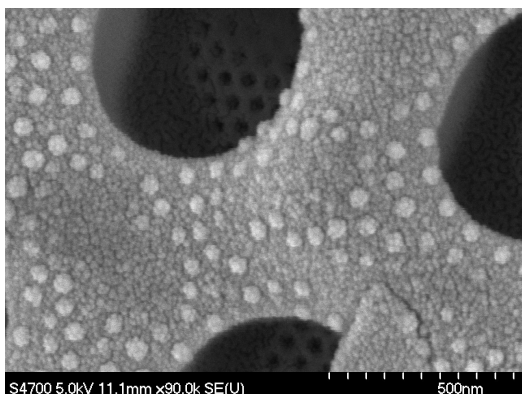
Figure 29: Higher magnification SEM image of 6 minutes of gold growth on a *T. eccentrica diatom.*
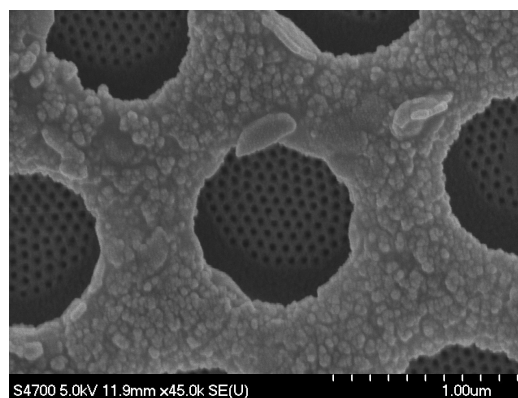
Figure 30: Overgrowth of gold under 3 minutes of coating on a *T. eccentrica* diatom. There is no evidence of ordered arrays of nanoparticle growth.

regular or interesting as the *Thalassiosira* species. Namely, the gold seemed to fill in the pores on the surface, rather than coating the sharp protrustions at the surface desired.

Neither *Thalassiosira decipiens* nor *Thalassiosira weissflogii* seem to form regular nanostructures under coating.

3.2 Atomic Force Microscopy of Supported Gold Nanostructures

The *T. eccentrica* standard diatom was imaged using the AFM such that gold nanostructures could be observed to grow with sputtering time.

AFM was used to image the diatoms prior to coating. See Figures 31, 32, and 33. Depressions in the surface of the foramen (Figure 32) were observed on the surface of the foramen prior to coating.

The AFM was then used to image the first stage of gold growth. AFM imagery of 30 seconds of the *T. eccentrica* standard diatom are included in Figures 34, 35, and 36.

Cribum imaging with AFM is very limited due to the width of the AFM tip. For example, in Figure 31, the AFM gives a ficticious triangular profile for the aereolae (the true shape of the aereolae is as indicated in Figure 3). This is due to the triangular shape

27
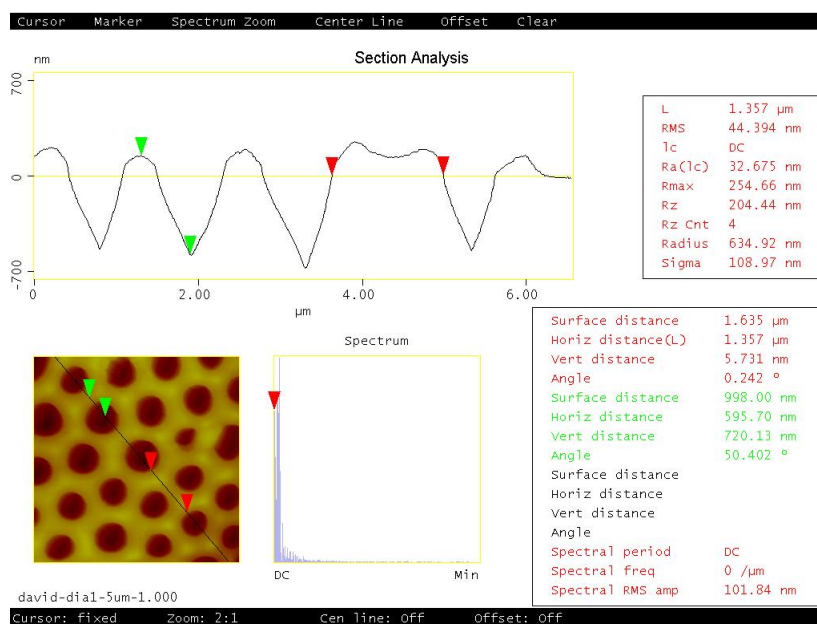
Figure 31: AFM imagery of the foramen of an uncoated *Thalassiosira eccentrica*. The AFM tip is limited in its ability to reach the sieve plate, giving a false triangular shape of the aereolae.

of the AFM tip, which is hitting the side of the foramen before reaching the cribum, giving this triangular profile. Because of this, unfortunately, it was not possible to image the surface of the cribum via AFM.

York River diatoms were also imaged using the AFM, but never with the *Thalassiosira* species of interest.

3.3 Energy-Dispersive Spectroscopy

Energy-dispersive spectroscopy (EDS) of an uncoated *T. eccentrica* diatom from culture was conducted. As expected, and confirming that the diatom was well cleaned, it is dominated by silicon and oxygen from the frustule, as well as carbon presint in the sample tab. See Figure 37.

Unfortunately, although EDS gives a good survey of elements in the SEM scan area, it does not have sufficient spatial resolution to determine composition on the scale of
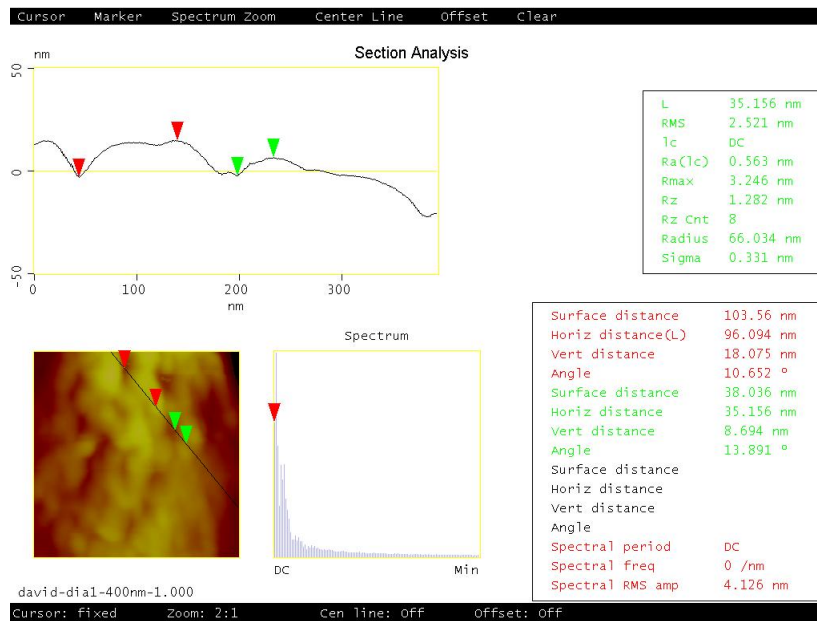
Figure 32: Close up (400 nm x 400 nm) scan of the foramen of the *T. eccentrica* standard diatom under no coating. Depressions in the foramen surface here likely act as nucleation sites upon coating. Compare this image with AFM imagery from [24] included in Figure 40.

Digital Instruments NanoScope
Scan size   3.000 µm
Scan rate   0.7266 Hz
Number of samples   512
Image Data   Height
Data scale   1.0000 um
Engage X Pos
Engage Y Pos

view angle
light angle

µm

2

1

0 °

X 1.000 µm/div
Z 1000.000 nm/div

david-dia1-3um-1.000
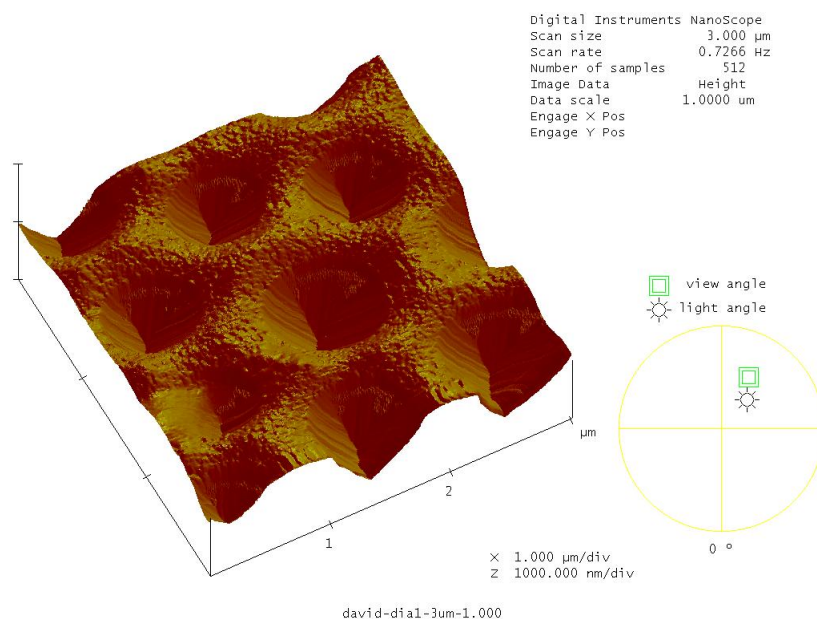
Figure 33: 3D projection of the AFM scan of the foramen of the *T. eccentrica* standard diatom with no coating. Compare this image with that of the coated diatom in Figure 34.

gold nanoparticles. Further attempts to use EDS to map the locations and distribution of the gold nanoparticles were not successful.

3.4 Carbon

Previous work demonstrated that the York River *Thalassiosira* form regular arrays of nanoparticles under carbon evaporation similar to thoses seen in gold sputter coating (See Figure 38). I also coated these supported carbon nanoparticle structures in gold. The resulting hybrid material retained the nanoparticle array structure (See Figure 39). Carbon evaporation was not done on the monoculture of *T. eccentrica*.

```
Digital Instruments NanoScope
Scan size          3.000 μm
Scan rate          1.071 Hz
Number of samples     512
Image Data         Height
Data scale         1.000 um
Engage X Pos
Engage Y Pos
```

view angle
light angle

μm

2

1

X   1.000 μm/div
Z   1000.000 nm/div

0 °

david-dia2-3um-1.000
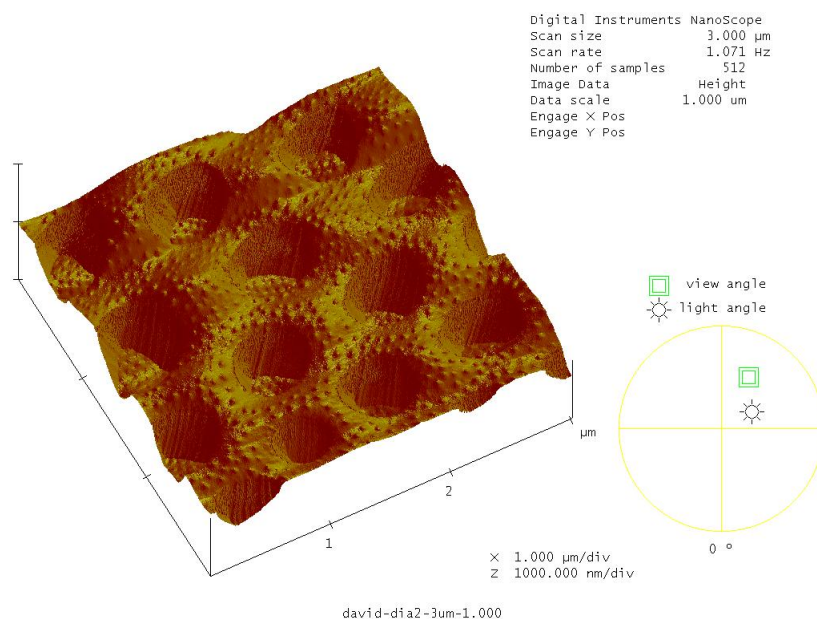
Figure 34: 3D projection of the AFM scan of the foramen of the *T. eccentrica* standard diatom with 30 seconds of coating. There are regular protrusions at the surface of the foramen. Compare this image with that of the uncoated diatom in Figure 33.

4   Planned Experiments & Measurements

I will continue work on this project through the summer of 2015, with the eventual goal of publishing this finding before I leave William & Mary. There are a number of experiments that I would like to conduct in order to explore this method of production of supported nanostructures, particularly for usefulness in catalysis applications.

4.1   Sputter Deposition Rate

A longstanding issue has been that the actual deposition rate of the sputter coater was unknown. The deposition rate is reported by Hummer to be 20 angstroms per minute, although this deposition rate is in doubt, and another measurement was needed to assess the validity of this.

A quartz crystal thickness monitor was used to make this measurement. The thick-
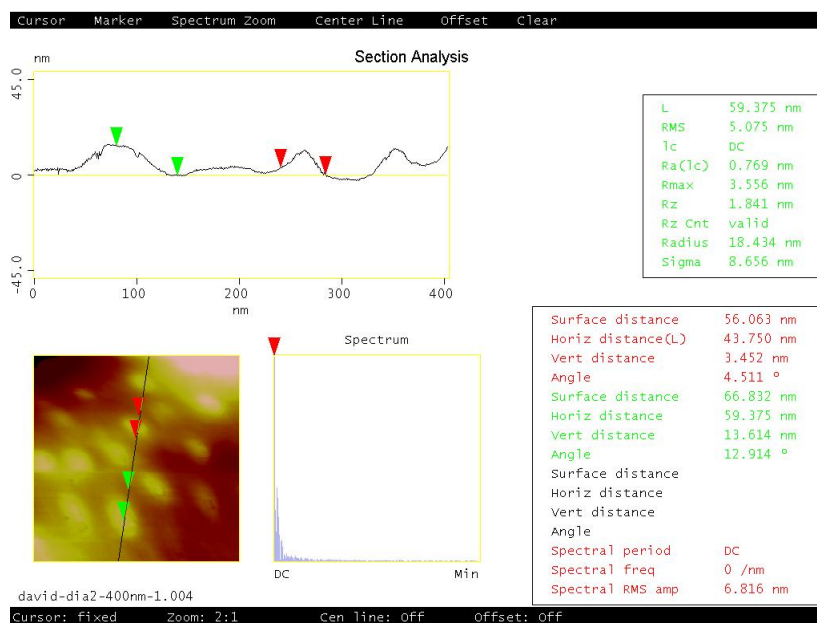
Figure 35: Close up (400 nm x 400 nm) scan of the foramen of the *T. eccentrica* standard diatom with 30 seconds of coating. Despite distortion of the image, nanoparticle formation is visible.
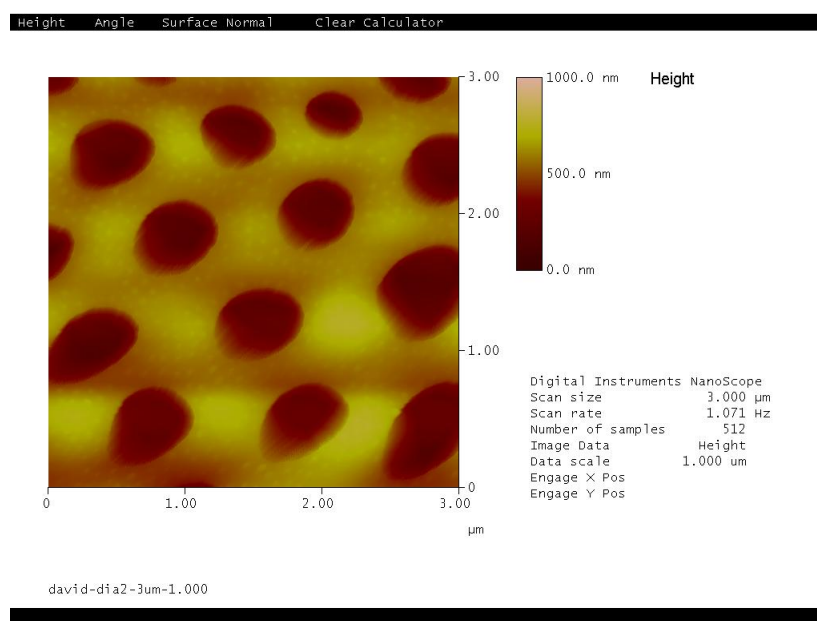
Figure 36: AFM scan of the foramen of the *T. eccentrica* standard diatom. Faint patterning visible here mirrors that seen in the SEM imagery: compare with Figure 26.

```
\\S-4700\bpr\David WM\04-14-15\Uncoated_TE.spc

Label:

kV:10.0 Tilt:0.0 Take-off:30.4   Det Type:SUTW+ Res:131 Amp.T:102.4

FS : 179  Lsec : 147                          7-Jan-1980 22:48:45
```
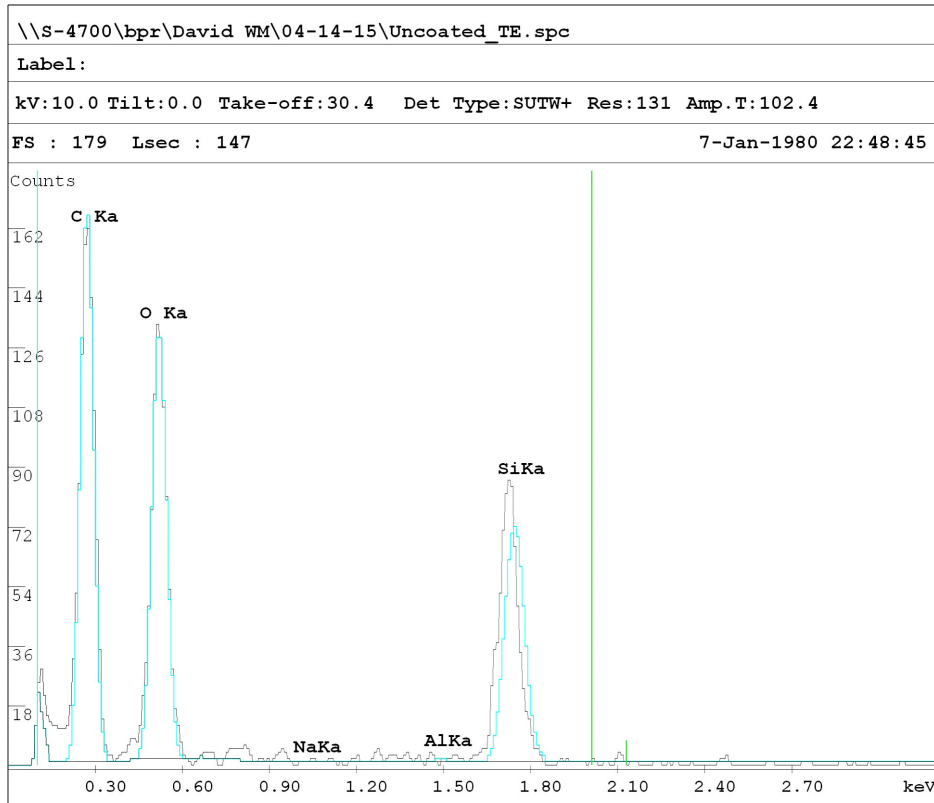
EDAX ZAF Quantification (Standardless)
Element Normalized
SEC Table : User c:\edax32\eds\genuser.sec

Element	Wt %	At %	K-Ratio	Z	A	F
C K	56.65	66.68	0.2736	1.0168	0.4748	1.0002
O K	30.23	26.71	0.1162	0.9942	0.3866	1.0001
NaK	0.00	0.00	0.0000	0.9204	0.7300	1.0011
AlK	0.19	0.10	0.0016	0.9091	0.9145	1.0050
SiK	12.92	6.51	0.1156	0.9344	0.9573	1.0000
Total	100.00	100.00				

Figure 37: EDS of an uncoated *T. eccentrica* diatom.
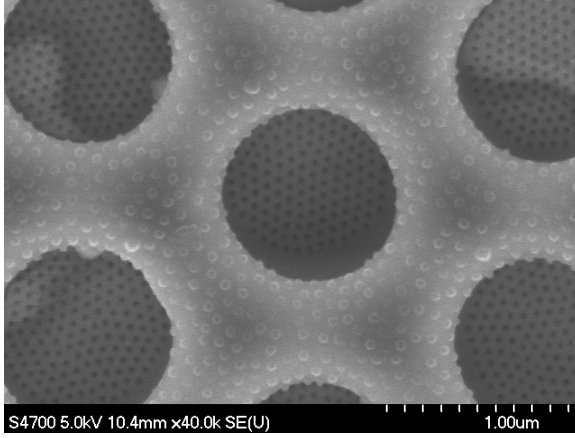
Figure 38: Growth of nanoparticles under carbon evaporation on a York River *Thalassiosira* diatom.
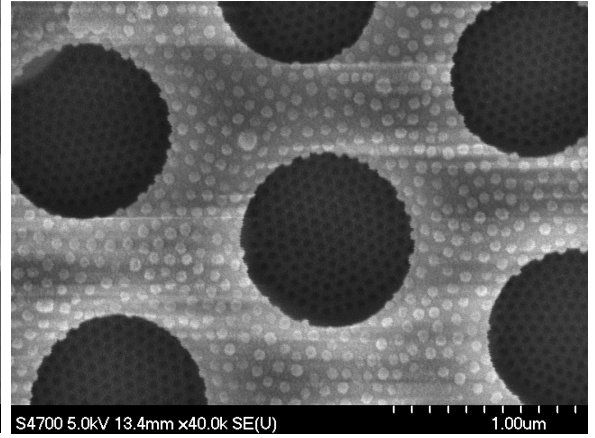
Figure 39: 40 seconds of sputtered gold on the supported carbon nanoparticles on a York River *Thalassiosira* diatom.

ness monitor works by measuring the alteration of the resonant frequency of a quartz crystal as material is deposited on the crystal surface [22]. The fundamental frequency is given by:

$$f = v_d/2d_q \tag{1}$$

where v_d is the elastic wave velocity and d_q is the plate thickness. For a film mass m, deposition area A, and film density ρ_f, the film thickness is given by:

$$d = m/A\rho_f \tag{2}$$

Combination of these two equations for a differential mass dm gives:

$$df = -\frac{f^2}{C\rho_f}\frac{dm}{A} \tag{3}$$

for frequency constant $C = v_q/2$ which is 1656 kHz-mm for cut quartz. For a small accumulated mass, df varies linearly with dm. Thus, the accumulated mass may be

measured using the alteration of this frequency.

4.2 Catalysis Measurement of Bulk Diatomaceous Material via Spectrophotometry

There are standard procedures for assessment of the catalytic capability of gold nanostructures, one of which uses reduction of 4-nitrophenol to 4-aminophenol in the presence of sodium borohydride as a reducing agent [23]. This is used, for example, in the assessment of the catalytic capability of gold diatom replicas [2]. The rate of change to 4-aminophenol is measured via spectrophotometry. The concentration of the resulting product can be measured by absorption spectroscopy and application of the Beer Lambert Law $A = \epsilon l c$ where where A is the measure of absorbance ($A = -log(I_{transmitted}/I_0)$), ϵ is the absorption coefficient, l is the path length, and c is the concentration, where intensity falls exponentially such that $I = I_0 e^{-\epsilon l c}$.

Large volumes of dried samples have been collected from the York River Algae Project raft, representing a wide variety of algae. I would like to sputter-coat a volume of this material, and use the above method to assess the catalytic potential of the resulting product. In particular, I would like to compare it to the fully templated structures described in [2].

This experiment aims to more directly address the question of what to do with the volumes of silica ash product resulting from pyrolization of diatomaceous algae for biofuel production, rather than study the impact of the morphologies of particular diatoms on catalytic capability. It may be interesting to see if this method is effective for other cheaper metals (e.g. iron), which also exhibit catalytic potential but are better suited for bulk scale production and use of the ash product.

4.3 Electrocatalytic Measurements of Diatomaceous Catalysts

Although the above method may be an excellent way to assess the bulk catalytic capabilites of diatom-templated gold nanostructures, it may not be well suited for low

volumes of material, or for study of how diatom morphology affects catalytic capability. Electrocatalysis, which is a form of catalysis that functions at electrode surfaces, can be measured at the microscopic level. I have met with Dr. McNamara in the chemistry department, who may be able to help me make such a measurement.

5 Discussion & Conclusions

In this work, I have demonstrated that *Thalassiosira eccentrica* can be used to template arrays of gold nanoparticles. Rather than uniformly coating the surface of the diatom frustules, sputtered gold will nucleate at at regular sites on the diatom surface and grow into larger nanoparticles. These have sizes ranging from 30 to 50 nm and occur at semiregular intervals. It is likely that these structures may have interesting applications, particularly in the area of nanocatalysis.

It seems that depressions (See Figure 32) in the foramen are acting as nucleation sites for the sputtered gold. Gold ions impinging on the surface will preferentially nucleate at these sites, and subsequent ions will preferentially form around these sites. However, the silica surface is not clearly different than AFM imagery from other species of diatoms. For example, AFM work done with a *Coscinodiscus sp.* diatom [24] shows similar silica growth (Compare Figure 40 from [24] with Figure 32). It remains somewhat mysterious why this growth phenomenon seems unique to certain *Thalassiosira* diatoms.

AFM imagery of the particles (Figures 35, 34, 36) seem to answer a longstanding question about the nature of the 'particles' visible in the SEM. Prior to work with the AFM, it wasn't certain that there were 'gold particles.' Rather, there was the possibility that the gold simply uniformly coated the surface, bringing out existing 'bumps' such that they were more illuminated in the SEM. However, there is clear growth of 'particles' between the uncoated and coated stages in the AFM (especially comparing Figures 33 and 34).
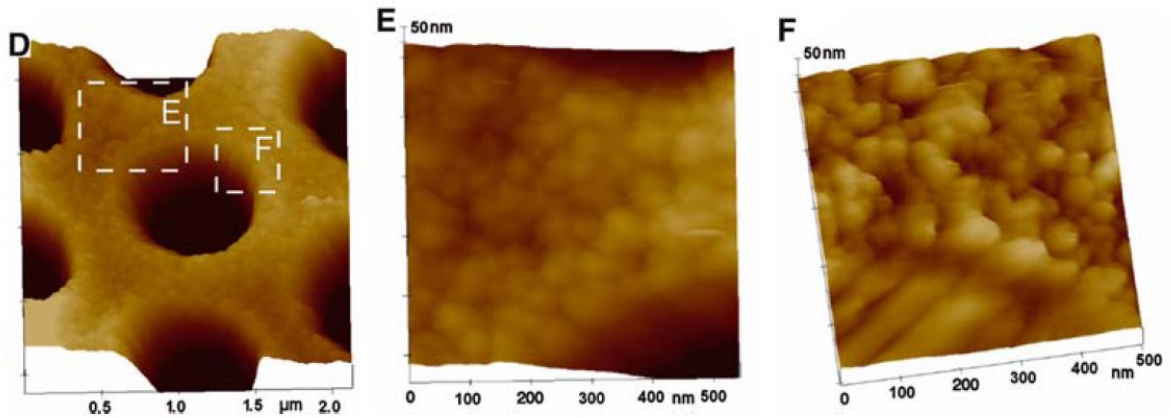
Figure 40: Image of the silica surface of the foramen of a *Coscinodiscus* diatom from [24]. Compare with Figure 32.

Nanoparticles had been previously observed to grow on the cribum of York River *Thalassiosira* species (e.g. Figure 2), and were measured to be about 10 nm in size. Particles were not observed to form on the cribum of the *T. eccentrica* diatoms.

More work needs to be done to explore the 'embryonic' conditions of when the particles first form. It is extremely difficult to image the frustules with small quantities of gold coating in the SEM, so this work will need to be done with the AFM. As it stands, it seems unlikely that the AFM will be able to resolve such growth very well. There is room for experimentation with improved security of frustules to the substrate or different AFM tips, which may improve the AFM resolution.

The new sample holder which allowed me to switch between the AFM and SEM for the same samples was very valuable. As expected, SEM image quality increases with gold coating. The ability to switch between to AFM imaging for the minimally coated samples compensated for the poor SEM resolution of these samples, and allowed me to have a better understanding of the particles when they first formed. It was particularly valuable to be able to return to the same diatom between coatings.

However, there is some interesting disparity between the AFM and SEM imagery of the uncoated diatoms. Namely, although there are depressions visible on the foramen

surface prior to coating with the AFM, they do not seem to be as highly ordered as the patterning viewable in the SEM (of both coated and uncoated samples). From the EDS of uncoated diatoms (Figure 37), it seems that the frustules are entirely silica and there aren't clearly and impurities present. There thus seems to be some ordered structure in the silica that causing even the uncoated sample to be illuminated in these locations.

There are some subtle differences between the York River *Thalassiosira* and the *T. eccentrica* (Compare, for example, Figures 23 and 24). The aerolae in the York River *Thalassiosira* species are significantly larger, with a larger portion of the cribum exposed as a result. The York River *Thalassiosira* also seems to have a much narrower girdle band, as they are never observed to lie on their sides (*T. eccentrica* frequently are observed to settle like this). Although the two are morphologically similar, and share a similar response to coating, I am inclined to believe that they are different species (or, more likely, that *T. eccentrica* describes many similar species of diatom).

Evaporation using carbon demonstrates the same affinity for production of these structures. It seems remarkable that both of these materials seem to show the same effect. This is indicative that this procedure may work for a whole variety of different materials. As demonstrated by the gold-coated carbon nanoparticle structure, it may be possible to create hybrid or multilayered materials that have this array of nanoparticles. I think that it is exciting that these diatoms could function as a 'universal template' for the production of arrays of size-controllable nanoparticles. Such unviersal templates, which can be inexpensively produced en masse, could have diverse nanotechnological applications.

Analysis of EDS of the uncoated diatoms didn't really reveal anything unexpected about their composition. It is possible that either the XRF or TOF-SIMS may reveal information about this. In particular, it may be interesting to know what non-silica compounds are taken up into the frustule, and if the situation of these plays some role in the frustule morphology.

These nanostructured materials already show great promise as supported gold catalysts. Production of these gold nanoparticles represents a novel and efficient means to distribute gold on a surface in an easy, one-step process. These supported nanoparticle arrays are likely more cost- efficient and effective than whole diatom replicas like those described in [2], for example. By templating metallic nanostructures from the diatom itself, but keeping the diatom itself as a support structure, one can efficiently use the gold and take full advantage of the diatom's intricate morphology.

Although this project has focused primarily on *T. eccentrica* diatoms, throughout this project I have also studied many other frustules with diverse morphologies. I think that it is extremely likely that these and many (tens of thousands) other diatom species may produce interesting structures under coating.

For example, the *Odontella* diatoms (Figures 11 and 12) have fascinating surface features, dominated by sharp protrustions on the valve face. Although these did not seem to coat under sputter-coating, it is entirely possible that a different deposition technique (e.g. electroplating) may be able to coat these structures and produce an interesting result of some kind.

It is not precisely clear how this project will or could help the York River Algae Project. Perhaps, if it is discovered precisely what is causing this phenomenon, it may be possible to use a wider variety of diatoms to produce a similar effect. Although the *Thalassiosira* species of interest is relatively sparse, certain diatoms (*Berkeleya sp.* and *Melosira sp.*) can be harvested in near-monoculture from the York River. It possible that if these are found to produce a similar effect, and with size-selection, the waste ash material could be used in this fashion. Coating this bulk frustule material in an inexpensive metal that has catalytic or other applications may produce a high-value application for this former waste product.

One application that these nanoparticle-decorated diatoms may be useful for is Surface-Enhanced Raman Scattering (SERS). Arrays of nanospheres are useful in this

application, and it is resonable that supported 'half-spheres' produced in this fashion may produce some similar effect. Nanoparticle decorated diatoms have previously been explored for applications in SERS (e.g. see [26]).

Another application could be use of the frustules as universal templates for production of nanoparticles from various materials. Despite the large number of potential applications, bulk production of many metallic nanoparticles above the milligram scale remains elusive. Diatom frustules are ideal templates, since they can be grown quickly and cheaply, and the nanoparticle growth phenomenon has already been demonstrated in this work with *T. eccentrica* for at least two materials. The template could then be removed via dissolution or etching (as in [2]), and the target particles could be isolated using established size-selection techniques. This method promises to be a very scalable method to produce bulk quantities of size-controlled nanostructures of potentially any material that can be sputtered or evaporated.

This particular phenomeon on this one diatom is representative of a whole array of possible biomimetic templates. Diatoms alone have some 200,000 species [8]. Diatoms are certainly not alone in that there are many other species that biomineralize nanostructured materials. It may be possible that a bank of many frustules and other biomineral templates could be kept and used to template a variety of nanostructures on-demand. Production of some new nanostructure in a new material could then be "data mining" [3] of new morphologies of nanostructures from existing templates, rather than figuring out new syntheses.

Arrays of nanoparticles grown using *T. eccentrica* represent a fascinating and unexpected origin of ordered nanomaterials from a biological template that may also have interesting and diverse applications. This frontier of biomimetic templates is as of yet insufficiently explored, and the tremendous morphological diversity of living materials may yield many more suprising phenomena. Use of diatomaceous algae as biomimetic templates stands to be a powerful technique to produce intricate nanomaterials.

6 Acknowledgements

I owe a huge debt of thanks to those who have helped me complete this project. This thesis is the result of several years worth of work, and there have been many people who have assisted me along the way. I would like to thank my advisor, Bill Cooke, as well as Dennis Manos, who has a longstanding interest in this subject. This project would not have been possible without the facilities available to me at the Applied Research Center Surface Characterization Laboratory. I would like to thank those at the Surface Characterization Lab who have spent many hours assisting me (Brandt Robertson, Olga Trofimova, Amy Wilkerson, Nick Moore, and Reed Beverstock). Brandt and Olga have spent enormous amounts of time on the SEM and AFM, respectively, and put up with some of my more absurd requests (like finding individual diatoms amid a sea of hundreds). I would like to thank Randy Chambers, for allowing me to use his spectrophotometer, and for agreeing to be on my committee. The species identification of *T. eccentrica* by Andrew Alverson enabled regular production of this phenomenon and made the final emphasis of this thesis on its study possible. I would also like to thank Holly Carlson, who helped me to develop the cleaning process for the frustules.

References

[1] Ryan Drum and Richard Gordon. Star trek replicators and diatom technology. *Trends in Biotechnology*, 21(8), 2003.

[2] Yang Yu, Jonas Addai-Mensah, and Dusan Losic. Synthesis of self-supporting gold microstructures with three-dimensional morphologies by direct replication of diatom templates. *Langmuir*, 26(17):14068–14072, 2010.

[3] Dusan Losic, James Mitchell, and Nicolas Voelcker. Diatomaceous lessons in nanotechnology and advanced materials. *Advanced Materials*, 2009.

[4] Dusan Losic, James Mitchell, and Nicolas Voelcker. Fabrication of gold nanostructures by templating from porous diatom frustules. *New Journal of Chemistry*, 30:908–914, 2006.

[5] Haiyan Li et al. Near-infrared selective and angle-independent backscattering from magnetite nanoparticle-decorated diatom frustules. *ACS Photonics*, 1:477–482, 2014.

[6] The chesapeake algae project: How environmental remediation can help solve our energy problem. `http://www.wm.edu/offices/economicdevelopment/_documents/100711vimschap.pdf`, October 10th, 2010.

[7] Dennis Manos. Final report de-ee0003146: Sustainable algal energy production and environmental remediation. Technical report, Department of Energy, 2013.

[8] Richard Gordon, Dusan Losic, Mary Ann Tiffany, Stephen S. Nagy4, and Frithjof A.S. Sterrenburg. The glass menagerie: diatoms for novel applications in nanotechnology. *Trends in Biotechnology*, 2008.

[9] Dusan Losic, James Mitchell, and Nicolas Voelcker. Complex gold nanostructures derived from templating from diatom frustules. *ChemComm*, 2005.

[10] A. Jantschke, C. Fischer, R. Hensel, H.-G. Braun, and E. Brunner. Directed assembly of nanoparticles to isolated diatom valves using the non-wetting characteristics after pyrolysis. *Nanoscale*, 6, 2014.

[11] Committee on the Sustainable Development of Algal Biofuels. Sustainable development of algal biofuels in the united states. Technical report, National Academy of Sciences, 2012.

[12] U. Heiz and U. Landman, editors. *Nanocatalysis*. Springer, Berlin, Germany, 2007.

[13] Younan Xia, Yujie Xiong, Byungkwon Lim, and Sara Skrabalak. Shape-controlled synthesis of metal nanocrystals: simple chemistry meets complex physics? *Angewandte Chemie*, 48:60–103, 2009.

[14] Britt Hvolbaek, Ton Janssens, Bjerne Clausen, Hanne Falsig, Claus Christensen, and Jens Norskov. Catalytic activity of au nanoparticles. *Nano Today*, 2(4):14–18, 2007.

[15] Erik Dreaden, Megan Mackey, Xiaohua Huang, Bin King, and Mostafa El-Sayed. Beating cancer in multiple ways using nanogold. *Chem. Soc. Rev.*, 40:3391–3404, 2011.

[16] Samual Lohse, Jonathon Eller, Sean Sivapalan, Michael Plews, and Catherine Murphy. A simple millifluidic benchtop reactor system for the high-throughput synthesis and functionalization of gold nanoparticles with different sizes and shapes. *ACS Nano*, 7(5):4135–4150, 2013.

[17] Avelino Corma and Hermenegildo Garcia. Supported gold nanoparticles as catalysts for organic reactions. *Chemical Society Reviews*, 37:2096–2126, 2008.

[18] Greta Fryxell and Greth Hasle. Thalassiosira eccentrica (ehrenb.) cleve, t. symmetrica sp. nov., and some related centric diatoms. *Phycology*, 8:297–317, 1972.

[19] Lisa M. Weimer. Chesapeake bay diatoms. Technical report, USGS, 1999.

[20] R.R.L Guillard. *Culture of Marine Invertebrate Animals*. Plenum Press, 1975.

[21] JC Taylor, WR Harding, and CGM Archibald. A methods manual for the collection, preparation and analysis of diatom samples. Technical report, Water Research Commission, 2007.

[22] Milton Ohring. *The Materials Science of Thin Films*. Academic Press, Inc., 1250 Sixth Avenue, San Diego, CA.

[23] Sudipa Panigrahi, Soumen Basu, Snigdhamayee Praharaj, Surojit Pande, Subhra Jana, Anjali Pal, Sujit Kumar Ghosh, and Tarasankar Pal. Synthesis and size-selective catalysis by supported gold nanoparticles: Study on heterogeneous and homogeneous catalytic process. *J. Phys. Chem. C*, pages 4596–4605, 2007.

[24] Dusan Losic, Rachel J. Pillar, Thorsten Dilger, James G. Mitchell, and Nicolas H. Voelcker.

[25] Peter Yunker, Zexin Zhang, and A. G. Yodh. Observation of the disorder-induced crystal-to-glass transition. *Physical review letters*, 104, 2010.

[26] Fanghui Ren, Jeremy Campbell, Xiangyu Wang, Gregory Rorrer, and Alan Wang. Enhancing surface plasmon resonances of metallic nanoparticles by diatom biosilica. *Optics Express*, 21, 2013.